Electronic Journal of Biotechnology 78 (2025) 96–109

Contents lists available at ScienceDirect

Electronic Journal of Biotechnology

journal homepage: www.elsevier.com/locate/ejbt

Research article

Kaixin San in treating vascular dementia via regulating the Bcl-2/Beclin-1/LC3A/B signaling pathway via animal experiments and network pharmacology analysis ☆

Meng-qi Li [a,1], Yu-cheng Lu [a,1], Yan-chun Li [a,1], Yu-fu Zeng [a], Ying-ying Cao [a], Ling Zhang [a,b,c,*], Ben Chen [a], Ling Chen [a], Wei-an Qiu [a], Zi-heng Huang [a]

[a] Institute of Traditional Chinese and Zhuang-Yao Ethnic Medicine, Guangxi University of Chinese Medicine, 530200 Nanning, China
[b] Guangxi Health Commission Guangxi Key Laboratory of Molecular Biology of Preventive Medicine of Traditional Chinese Medicine, 530024 Nanning, China
[c] Guangxi Key Laboratory of Chinese Medicine Foundation Research, Guangxi University of Chinese Medicine, 530200 Nanning, China

GRAPHICAL ABSTRACT

Kaixin San in treating vascular dementia via regulating the Bcl-2/Beclin-1/LC3A/B signaling pathway via animal experiments and network pharmacology analysis

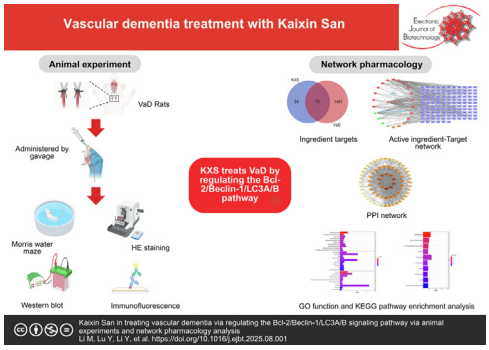

ARTICLE INFO

Article history:
Received 28 May 2025
Accepted 11 August 2025
Available online 15 October 2025

Keywords:
Bcl-2/Beclin-1/LC3A/B
Kaixin San
Morris water maze test
Network pharmacology analysis

ABSTRACT

Background: Kaixin San (KXS), a traditional Chinese herbal formula, is used to treat vascular dementia (VaD), but its active ingredients and mechanisms remain unclear. This study combined animal experiments with network pharmacology to explore how KXS modulates the Bcl-2/Beclin-1/LC3A/B pathway in VaD treatment.

Results: LC MS/MS identified 164 active ingredients in the KXS ethanol extract. In 2-vessel occlusion model rats, KXS significantly improved learning and memory ($p < 0.05$ or $p < 0.01$) and reduced hippocampal CA1 neuronal damage. Western blotting showed KXS upregulated Bcl-2/Bcl-XL and downregulated Beclin-1, LC3A/B, and Bax ($p < 0.05$). Immunofluorescence confirmed increased Bcl-2 and decreased Beclin-1 expression. Network pharmacology predicted 73 targets and 174 pathways, with

Abbreviations: GO, Gene Ontology; KXS, Kaixin San; KCP, KXS combined with piracetam; KEGG, Kyoto Encyclopedia of Genes and Genomes; PPI, Protein–Protein Interaction; VaD, Vascular dementia.

☆ Audio abstract available in Supplementary material.

Peer review under responsibility of Pontificia Universidad Católica de Valparaíso.

* Corresponding author.
E-mail address: 754664650@qq.com (L. Zhang).

[1] These authors contributed equally to this work.

https://doi.org/10.1016/j.ejbt.2025.08.001

Signaling pathway
Vascular dementia

TNF, AKT1, IL-1β, PTGS2, and ESR1 as key targets. Kyoto Encyclopedia of Genes and Genomes (KEGG) analysis linked these targets to cancer, atherosclerosis, and AGE-RAGE signaling pathways.
Conclusions: KXS alleviates VaD by modulating autophagy and apoptosis via Bcl-2/Beclin-1/LC3A/B, with multi-target, multi-pathway effects. These findings support further investigation of KXS as a potential therapy for VaD.

How to cite: Li M, Lu Y, Li Y, et al. Kaixin San in treating vascular dementia via regulating the Bcl-2/Beclin-1/LC3A/B signaling pathway via animal experiments and network pharmacology analysis. Electron J Biotechnol 2025;78. https://doi.org/10.1016/j.ejbt.2025.08.001.

1. Introduction

Vascular dementia (VaD) is a syndrome of impaired cognitive function caused by cerebrovascular disease, which usually presents with symptoms such as memory loss, impaired cognitive capacity, language impairment and movement impairment [1,2]. Owing to the aging population of society, its incidence is increasing annually, making it the second most common form of dementia after Alzheimer's disease [3,4]. At present, there is no specific drug for the treatment of VaD in clinical practice, which has caused severe economic burdens to patients and society [5].

Kaixin San (KXS) was first recorded in Sun Simiao's Beiji Qianjin Yao Fang, which has the functions of nourishing the heart and calming the mind, benefiting the intellect and strengthening the brain, dispelling phlegm and opening orifices. *Poria*, *Ginseng Radix et Rhizoma*, *Polygalae Radix* and *Acori Tatarinowii Rhizoma* are included in the medicine prescription [6]. In this formula, *Poria* is used as the principal medicine, which can clear dampness and promote diuresis; *Ginseng Radix et Rhizoma* can calm the mind and improve cognition; *Polygalae Radix* can eliminate phlegm and open orifices; and the two are used as minister medicines. *Acori Tatarinowii Rhizoma* is used as an assistant medicine that benefits the intellect and open orifices [7]. In Chinese medicine, VaD mainly occurs in the brain, with blood stasis and phlegm turbidity as the main pathogenic factors. Therefore, the main treatment for this disease is tonifying the kidney and essence, arousing the brain and nourishing marrow, reducing phlegm and activating blood circulation to achieve the functions of opening orifices and strengthening the brain [8]. This study explored the effect and mechanism of KXS on VaD.

Modern clinical applications and experimental studies have proven the positive pharmacological effects of KXS on dementia prevention and antioxidation [9]. However, the pathophysiology of VaD is complex and is often thought to be associated with oxygen radical damage, inflammatory responses and excitatory amino acid toxicity [10]. Inhibiting autophagy and apoptosis in neuronal cells is a key way to prevent and improve VaD [11]. Therefore, to verify this hypothesis, a study was conducted to establish a VaD model by applying 2-vessel occlusion to observe the improvement effect of KXS and further explore its mechanism, with the goal of providing an experimental basis for the prevention and treatment of VaD in Chinese medicine as well as the clinical application of KXS.

2. Materials and methods

2.1. Main reagents and instruments

Poria was purchased from Beijing Tongrentang Health Pharmaceutical (Fuzhou) Co., Ltd. (Hubei, China), *Ginseng Radix et Rhizoma* was purchased from Beijing Bencaofangyuan Pharmacy Group Ltd. (Jilin, China), *Polygalae Radix* was purchased from Tianjin Shengshi Pharmaceutical Co., Ltd. (Shanxi, China), and *Acori Tatarinowii Rhizoma* was purchased from Beijing Bencaofangyuan (Bozhou) Pharmaceutical Technology Co., Ltd. (Pingwu, Sichuan, China). Piracetam tablets were purchased from Yichang Humanwell Pharmaceutical Co., Ltd. (Hubei, China). An ultrasensitive ECL chemiluminescence kit was purchased from Beyotime Biotechnology (Shanghai, China). A BCA protein assay kit, SDS PAGE loading buffer (5 ×), prestained colored protein molecular weight marker and SDS PAGE gel preparation kit were purchased from Jiangsu KeyGEN Bio TECH Co., Ltd. (Jiangsu, China). GAPDH, LC3A/B, Beclin-1, Bcl-2, Bax, Bcl-XL and goat anti-rabbit IgG (HRP) were purchased from Abcam (Cambridge, UK).

Rotary Evaporator (Shanghai Ailang Instruments Co., Ltd., N-1300); MORRIS water maze video analyser system (ShangHai Biowill Co., Ltd., BW-MWM101); automatic dehydrator, Tissue Embedding Machine, Otary Wheel Slicer (Leica, ASP300S, ASP300S, HM355S); ultrahigh sensitivity chemiluminescence imaging system (Bó Lè Life Medical Products (Shanghai) Co., Ltd., Chemi DocTM XRS+); microplate readers (TECAN, INFINITE 200 PRO); inverted microscope (OLYMPUS CORPORATION, BX30053F); and QTOF mass spectrometer (SCIEX, X500R).

2.2. Ethanol extraction of KXS ingredients

KXS was recorded in Beiji Qianjin Yaofang by the Tang Dynasty physician Sun Simiao [6]. The formula composition in this study uses the modern dosage of: *Poria* (Fuling) 60 g, *Ginseng Radix et Rhizoma* (Renshen) 1.2 g, *Polygalae Radix* (Yuanzhi) 1.2 g and *Acori Tatarinowii Rhizoma* (Shichangpu) 30 g. The nine packets of herbal powder were uniformly mixed using the geometric dilution method. Subsequently, 60% ethanol was added at a 1:10 solid–liquid ratio. Ultrasonic extraction (Elma, Germany) was then performed for 30 min daily. After the preceding steps were finished, the liquid and residue were separated through filtration, the liquid was stored at 4°C, and the residue was mixed with 60% ethanol at a 1:8 ratio and steeped for 24 h. Next, all the liquid and residue were extracted for 4 h via the reduced pressure reflux method and then filtered via a vacuum pump (Zhengzhou Greatwall Scientific Industrial and Trade Co., Ltd., Henan, China). The liquid was concentrated under reduced pressure to 3 L in a rotary evaporator (Shanghai Ailang Instrument Co., Ltd., Shanghai, China), evaporated in a 60°C constant-temperature water bath (Shanghai Yiheng Technology Instrument Co., Ltd., Shanghai, China), and finally, a KXS ethanol extract was obtained. The resulting extract weighed 61.53 g.

2.3. Preliminary screening of the chemical constituents of the ethanol extract of KXS

A total of 10 mg of the KXS ethanol extract was accurately weighed and deposited in a 50 ml centrifuge tube. Ten milliliters

of 50% methanol aqueous solution was added to the centrifuge tube, ultrasonic extraction was performed for 30 min, and the tube was centrifuged for 5 min at 8000 rpm. The resulting solution was filtered through a 0.22 μm nylon microporous membrane and transferred to a 1.5 mL sample bottle for machine analysis. The chemical constituents of the KXS ethanol extract were screened and analyzed via a SCIEX high-resolution X500R QTOF LC/MS instrument. Gradient elution was performed with analytically pure methanol (A) and 0.1% (v/v) formic acid aqueous solution (B) with the following elution procedure: 5%A 0–0.5 min, 5–7%A 0.5–2 min, 7–25%A 2–4 min, 25–25%A 4–6 min, 25–30%A 6–8 min, 0–35%A 8–10 min, 35–40%A 10–14 min, 40–40%A 14–16 min, 40–50%A 16–17 min, 50–55%A 17–18 min, 55–60%A18–20 min, 60–70%A 20–24 min, 70–70%A 24–26 min, 70–75%A 26–31 min, 75–80%A 31–33 min, 80–85%A 33–35 min, 85–95%A 35–36 min, 95%-5%A 36–36.5 min, and 5%-5%A 36.5–40 min. The flow rate was 0.3 mL/min, and the injection volume was 5 μL [12].

2.4. Animals and subgrouping

All the animal experiments were reviewed and approved by the Guangxi University of Chinese Medicine Institutional Welfare and Ethical Committee, and all the studies were conducted in accordance with the United States Public Health Service's Policy on Humane Care and Use of Laboratory Animals. A total of 80 male Sprague-Dawley rats at 6 weeks of age weighing 180–220 g were purchased from Hunan Silaikejingda Experimental Animal Co., Ltd. (Animal Use Licence No. SYXK Gui 2019-0001, Laboratory Animal Production Licence No. SCXK Xiang 2019-0004, Approval No. DW20211210-205). The rats were housed at the Laboratory Animal Center of the Institute of Guangxi University of Chinese Medicine with free access to water and lab chow and were maintained under a 12 h light/dark cycle. Twenty rats were randomly selected for the control and sham groups (n = 10) via a randomized numerical table. In the sham group, the same surgical procedure was used as in the VaD model group, but neither of the bilateral common carotid arteries were occluded. In the VaD model group, the bilateral common carotid arteries were permanently occluded with nylon filaments [13]. Surgical exclusion criteria: animals were excluded if they failed to exhibit contralateral forelimb flexion or circling behavior 2 h post-modeling, or if they failed to regain consciousness. The survival rate of the surgery is approximately 70%. Successfully established rats were randomly divided into the VaD model group (n = 10), KXS group (n = 10), piracetam group (n = 11) and KXS combined with KCP group (n = 11).

2.5. Drug treatment

On the basis of the extraction rate and dose conversion relationship between humans and rats, the dosage of the KXS group was 0.06154 g/mL. The dosage for adults in the piracetam group was 0.0072 g/mL. The KCP group was gavaged with both drugs at the above doses. The rest of the samples were gavaged with equal amounts of 0.9% sodium chloride solution. The treatments were administered once daily for 4 weeks.

2.6. Morris water maze test

The test involves a circular water tank divided into four quadrants. An escape platform was placed in the center of the target quadrant and submerged approximately 1 cm below the water surface. The test lasted for 6 d, and the water temperature was maintained at 20 ± 5°C before training. During training, the rats were placed on the platform for 20 s to learn its location, after which they were gently released into the water facing the wall and then permitted to swim freely to find the hidden platform. The time necessary for rats to locate the escape platform within 120 s was recorded. If a rat failed to find the platform within 120 s, it was guided to the platform and allowed to stay there for 20 s. Each rat was tested twice a day starting from different quadrants, and the average value was used as the evaluation index. On the last day of the test, the escape platform was removed, and each rat was permitted to swim freely in the tank for 120 s. The time spent in the target quadrant and the number of times the rat crossed the original platform were recorded via a camera above the pool and calculated via a computer with a tracking system [14,15,16].

2.7. Sample collection and preparation

After the Morris water maze experiment, each rat was injected with 0.9% sodium chloride solution. Perfusion was completed when the rats' forelimbs and eyes were white. Half of the rats in each group were selected and decapitated for Western blotting, and the brain was immediately dissected via surgery on ice and frozen in liquid nitrogen at −80°C. The remaining rats were perfused with 4% paraformaldehyde as previously described for Hematoxylin and Eosin (HE) staining. When the limbs of the rats became stiff, the entire brain was removed and submerged in a paraformaldehyde solution for fixation.

2.8. HE staining

The brain tissue submerged in 4% paraformaldehyde solution was removed, cut into blocks, and then dehydrated with a Leica ASP300S fully enclosed tissue processor (Leica Biosystems Nussloch GmbH, Germany) for 15 h. After dehydration, paraffin embedding was conducted, and the sections were cut with a Leica Biosystems RM2245 semi-motorized rotary microtome (Leica Biosystems Nussloch GmbH, Germany) after they were frozen to a suitable hardness level. Finally, HE staining was applied to observe the morphological changes in the hippocampal CA1 cells in each group under a microscope (Olympus Corporation, Japan).

2.9. Western blot

The protein concentration was determined with a BCA protein assay kit. Protein samples were separated by 8–12% SDS–PAGE and transferred to polyvinylidene fluoride membranes. The membranes were blocked with 5% nonfat milk in Tris-buffered saline with Tween-20 for 1 h at room temperature and then co-incubated with primary antibodies separately at 4°C overnight. The antibodies used included anti-GAPDH (1:10,000; ab181602), anti-LC3A/B (1:1,000; ab128025), anti-Beclin-1 (1:1,000; ab210498), anti-Bcl-2 (1:2,000; ab182858), anti-Bax (1:1,000; ab32503), and anti-Bcl-XL (1:1,000; ab32370) antibodies. After being washed 3 times (10 min each time) with TBST, the membranes were incubated with horseradish peroxidase-conjugated secondary antibody (1:2,000, ab6721) at room temperature for 1 h. The protein bands were detected via an ultrasensitive ECL chemiluminescence kit and quantified via ImageJ software.

2.10. Immunofluorescence

Hippocampal tissue sections from each group of rats were processed as follows: After antigen retrieval, the sections were blocked for 1 h and subsequently incubated with Bcl-2 (1:200 dilution) and Beclin-1 (1:50 dilution) antibodies at 4°C overnight. Following primary antibody incubation, IgG secondary antibody (1:50 dilution) was applied and incubated at room temperature for 1 h under light-protected conditions. Nuclei were counterstained with

4′,6-diamidino-2-phenylindole (DAPI). Fluorescence microscopy was employed for image acquisition, and quantitative analysis of mean fluorescence intensity in the hippocampal neuronal cells was performed using ImageJ software.

2.11. Data analysis

Statistical visualization and analysis were carried out with GraphPad Prism software version 9.0 and SPSS software version 26. One-way ANOVA and the least significant difference (LSD) test were performed for comparisons of means between groups. *p*-values < 0.05 were considered statistically significant.

2.12. Identification of active ingredients and action targets

The parameters of oral bioavailability ≥30% and drug likeness ≥0.18 were set [17], and the ingredients and targets of *Poria, ginseng, Polygalae Radix, and Acori tatararinowii Rhizoma* were searched in the Traditional Chinese Medicine Systems Pharmacology Database (TCMSP) https://old.tcmsp-e.com/tcmsp.php). Finally, the UniProt database was used (https://www.uniprot.org) to obtain the short name of the gene corresponding to the target.

2.13. Collection of the VaD gene and crossing targets

Genes related to VaD diseases were collected from the GeneCards database (https://www.genecards.org) by inputting "vascular dementia" and setting the relevance score ≥4.35. The active ingredient action target set and VaD disease gene set were crossed to identify the potential target set of KXS for the treatment of VaD. Finally, the ingredient-target data of KXS for the treatment of VaD were obtained via bioinformatics and evolutionary genomics (https://bioinformatics.psb.ugent.be/webtools/Venn/).

2.14. Construction of the active ingredient-target network

The above ingredient target data were imported into Cytoscape (version 3.10.0) to construct the "active ingredient target" network. The higher the degree is, the larger the node of the compound and the darker the color of the target; at the same time, the greater the degree of association with other network nodes is, the more important that node in the network.

2.15. Construction of protein protein interaction (PPI) networks

First, the crossing targets were imported into the STRING database (https://string-db.org), the species was set as "*Homo sapiens*", the protein interaction threshold was set as "Highest confidence (0.900)", the discrete nodes were removed, and a PPI was constructed. The protein interaction information was subsequently imported into Cytoscape (version 3.10.0) for visualization and topological analysis.

2.16. Gene Ontology (GO) and Kyoto Encyclopedia of Genes and Genomes (KEGG) pathway enrichment analysis of targets

The Metascape database (https://metascape.org/gp/index.html) was used for the GO and KEGG analyses on crossing targets, with the species set to "*Homo sapiens*". The GO enrichment analysis included three aspects: biological processes, cellular ingredients, and molecular functions. The KEGG analysis screening conditions were set to a *p*-value <0.01. Weishenxin (https://www.bioinformatics.com.cn/) was used to visualize the results of the above analysis to screen the biological functions and signaling pathways of KXS in VaD.

3. Results

3.1. Chemical composition analysis of KXS

The chemical composition of KXS was analyzed using Exion LC AC liquid chromatography coupled with X500R QTOF mass spectrometry. A total of 164 compounds were tentatively identified, with the total ion chromatogram presented in Fig. 1. By cross-referencing MS/MS fragmentation patterns with relevant traditional Chinese medicine chemical constituent database resources, representative compounds including betulin, kaempferol, ginsenoside Rf, ginsenoside Rg1, rhein, purpurin, and ginsenoside Rh1 were characterized. The complete results are systematically compiled in **Table S1**.

3.2. Effects of KXS on the learning and memory ability of rats

As shown in Fig. 2A–E, the experimental results of directional navigation revealed that the escape latency of the rats in each group tended to decrease daily, and the escape latency of the VaD model group was longer than that of the other groups. On the first day of the experiment, the escape latency of the other groups was significantly shorter than that of the VaD model group ($p < 0.05$ or $p < 0.01$). As shown in Fig. 2F–G in the space exploration experiments, compared with the control group, the VaD model group spent less time in the target quadrant and crossed the platform ($p < 0.05$). Compared with those in the VaD model group, the rats in each treatment group stayed in the target quadrant longer and crossed the platform more often, and the difference was statistically significant ($p < 0.05$ or $p < 0.01$).

3.3. Effects of KXS on hippocampal neurons in rats

The morphology and structure of the neurons in the control group were normal. The shape of the neurons in the sham group was slightly deformed, and the degree of fullness and filling was weaker than that in the control group, but it was better than that in the VaD model group. Although the neurons in the VaD model group were tightly arranged, the morphology of the neurons was deformed, and the nuclei had shrunk. Compared with those in the VaD model group, the neurons in the KXS, piracetam and KCP groups were normal in morphology, structurally intact and tightly arranged, and improved (Fig. 3).

3.4. Effects of KXS on the expression of autophagy and apoptosis-related proteins in rat brain

As shown in Fig. 4, the expression levels of the autophagy-related proteins LC3A/B and Beclin-1 were elevated in the VaD model group compared with those in the control and sham groups, indicating that autophagy was increased in the brains of VaD model group rats. Compared with those in the VaD model group, the LC3A/B and Beclin-1 protein expression levels were significantly lower in each treatment group ($p < 0.05$ or $p < 0.01$), indicating that the drug inhibited the occurrence of autophagy in the brains of the rats. Compared with those in the control group and sham group, the expression levels of Bcl-2 and Bcl-XL in the VaD model group were decreased, whereas the expression levels of Bax were increased, suggesting increased levels of apoptosis in the brains of the VaD model group. Compared with those in the VaD model group, the expression levels of Bcl-2 and Bcl-XL in all the administration groups tended to increase, and the expression level of Bcl-XL in the KXS group significantly increased ($p < 0.05$), whereas the expression level of Bax in all the administration groups significantly decreased, and the difference was statistically

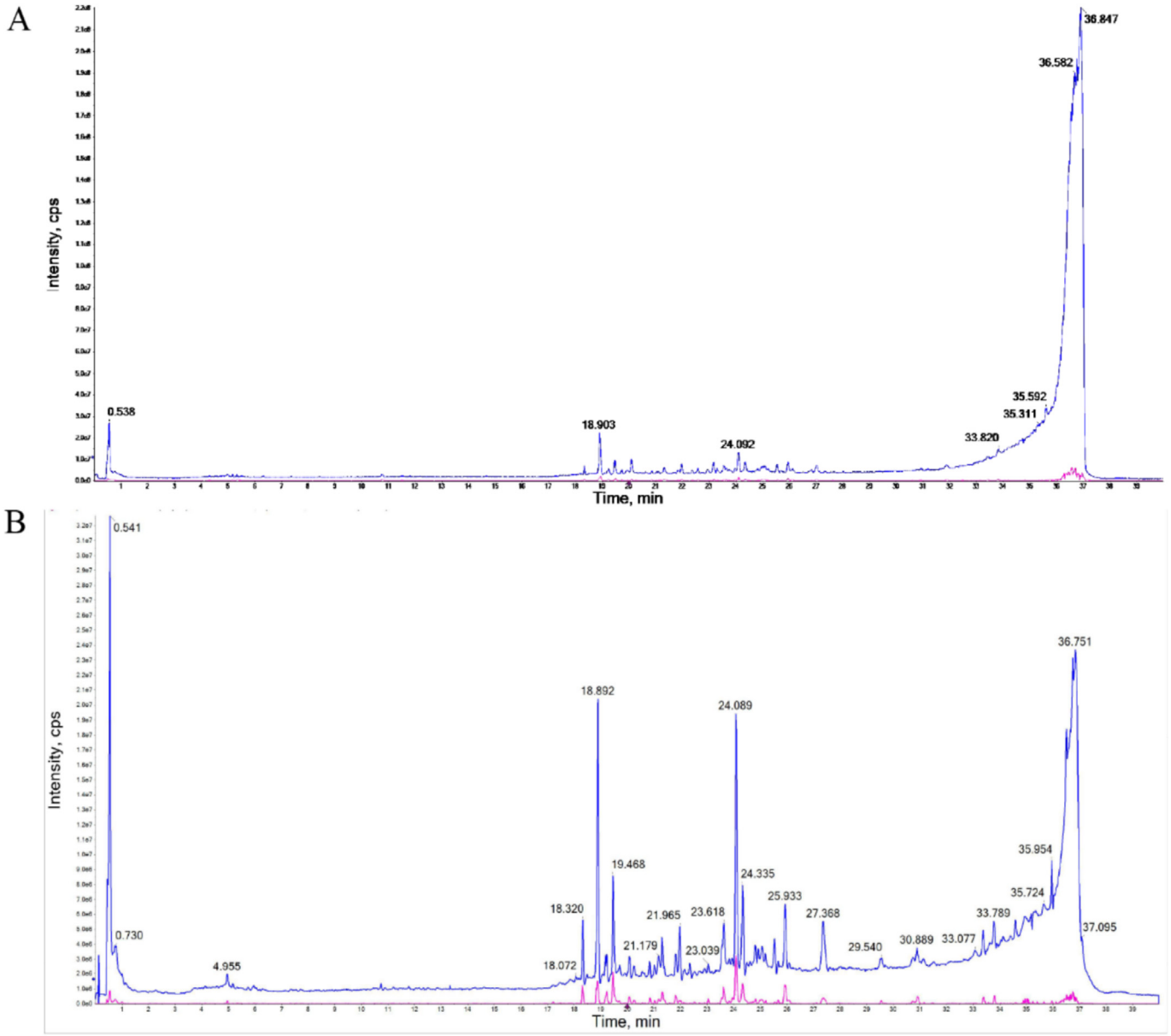

Fig. 1. Chemical compositions analysis of KXS. (A) Total ion flow diagram in positive ion mode; (B) Total ion flow diagram in negative ion mode.

significant ($p < 0.05$ or $p < 0.01$), which indicated that the drug was able to inhibit apoptosis in the rat brain.

3.5. Effect of KXS on expression of Bcl-2 and Beclin-1 in rat brain

Compared with the blank control group, the model group showed reduced fluorescence intensity of Bcl-2 and enhanced fluorescence intensity of Beclin-1 in rat hippocampal tissues. In comparison to the model group, all treatment groups demonstrated increased Bcl-2 fluorescence intensity accompanied by decreased Beclin-1 fluorescence intensity in the hippocampal tissues (Fig. 5).

3.6. Screening of the active ingredients and targets of KXS

The TCMSP database was used for screening, and 3 active ingredients and 25 targets for *Poria*, 22 active ingredients and 112 targets for ginseng, 2 active ingredients and 13 targets for *Polygalae Radix*, and four active ingredients and 77 targets for *Acori Tatarinowii Rhizoma were obtained*. After deleting repetitive ingredients, targets and those without therapeutic targets, 26 active ingredients and 127 targets of KXS were obtained. The basic information of the active ingredients is shown in Table 1. The GeneCards database was used to screen 1462 disease targets by setting the median relevance score ≥ 4.35. The intersection of the active ingredient target and the VaD disease-related target was used to obtain a total of 73 targets (Fig. 6).

3.7. Construction of the active ingredient–target network

Cytoscape 3.10.0 software was used to construct the "active ingredient target" network of KXS for the treatment of VaD, as shown in Fig. 7. In the network, the diamond node represents the active ingredients, the purple square node represents the target, and each edge represents the interaction between the active ingredients and the VaD-related target. There are interactions between active ingredients and multiple targets in the network, as well as

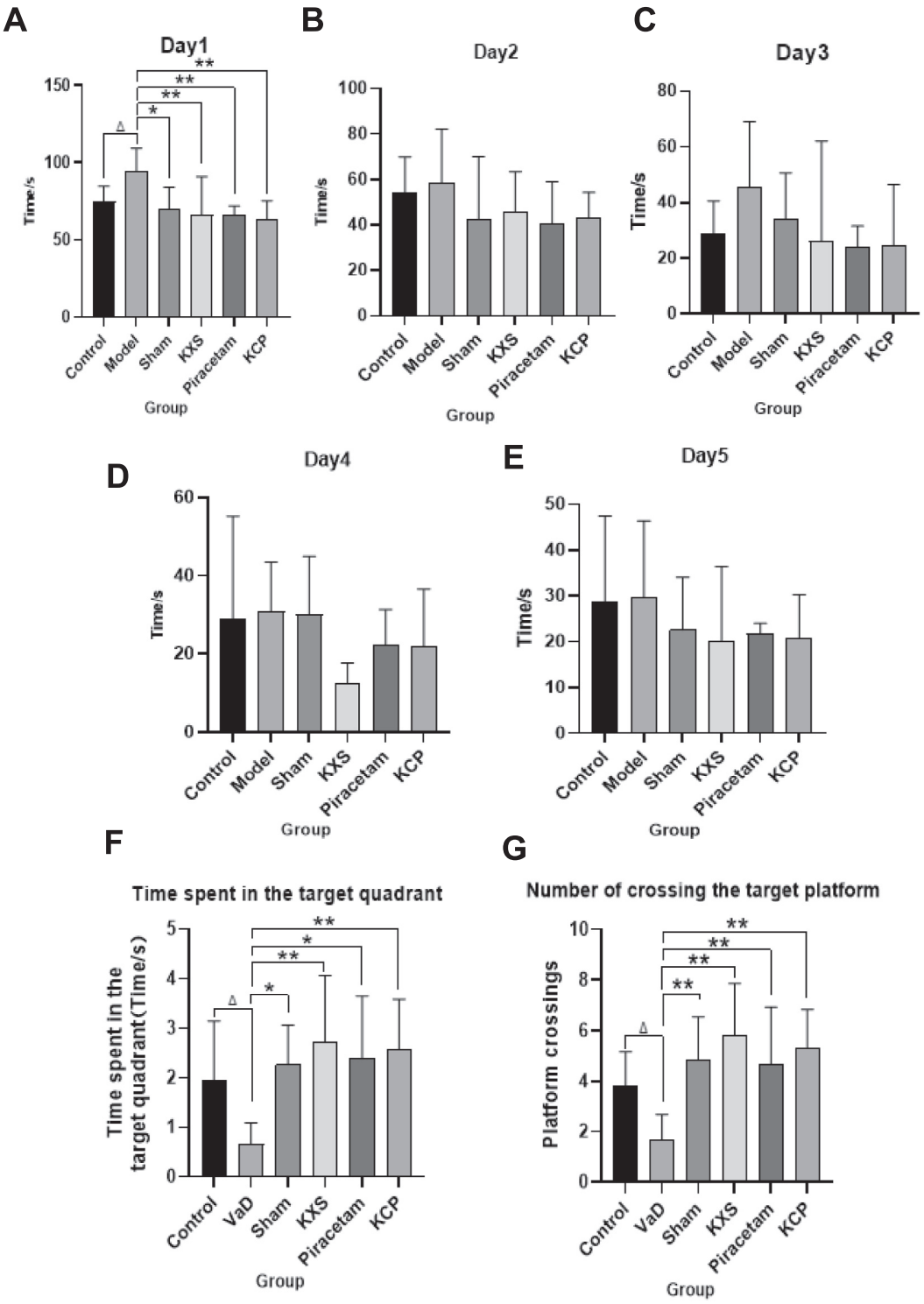

Fig. 2. Morris water maze test. (A-E). Time to escape the incubation period. (F) Time spent in the target quadrant. (G) Number of crossings the target platform. (Compared with the control group, $^{\Delta}$ indicates $p < 0.05$; compared with the VaD group, * indicates $p < 0.05$ and ** indicates $p < 0.01$).

different active ingredients interacting with the same target, reflecting the mechanism of action of the multi-ingredient and multitarget treatment of VaD by KXS.

3.8. PPI network construction and core target screening

The intersecting targets were uploaded to the STRING database, and the PPI network was constructed in "highest confidence (0.900)" mode with 123 nodes, 201 edges, an average node degree of 3.27, and a PPI enrichment *p*-value < 1.0e-16, as shown in Fig. 8. The network files obtained from STRING were input into Cytoscape 3.10.0 software and visualized according to their degree. The larger the graph is and the darker the color is, the larger the degree value is, which means that it is more important to the network. Among them, TNF, ATK1, IL-1B, PTGS2, ESR1, CASP3, PPARG, BCL2, JUN, TGFB1, etc., are the core targets of KXS for VaD treatment, as shown in Fig. 9.

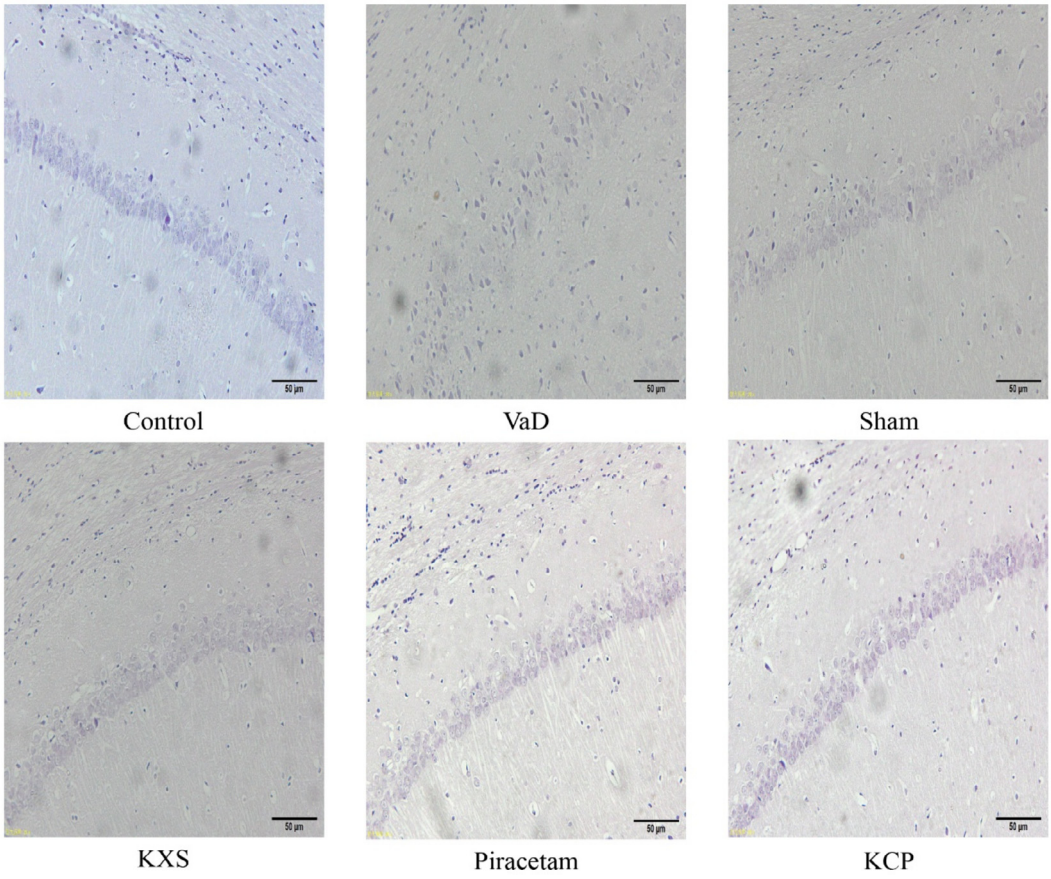

Fig. 3. Histopathological morphology of hippocampal neuronal cells.

3.9. Gene ontology enrichment analysis

A *p*-value < 0.05 was used as the filtering condition, and the top 10 results are displayed in Fig. 10. Biological process terms are as follows: response to xenobiotic stimulus, positive regulation of gene expression, positive regulation of apoptotic process, and so on. The cellular components (CCs) included mainly the plasma membrane, cytosol, and neuronal cell body. The molecular functions (MFs) included mainly protein binding, identical protein binding, and enzyme binding.

3.10. KEGG pathway enrichment analysis

A *p*-value < 0.05 was used as the filtering condition, 174 KEGG pathways were obtained, and the top ten pathways are listed in Fig. 11. The larger and darker color of the bubble map in the figure indicates that it is more important, which reveals that lipids and atherosclerosis, fluid shear stress and atherosclerosis, and pathways in cancer may be important for the treatment of VaD.

4. Discussion

Ginsenosides, the main active ingredients of ginseng, have been widely used in the study of nervous system diseases, myocardial ischemia reperfusion injury and other diseases [18,19]. It functions to protect neurons, regulate neurotransmitters and promote the apoptosis of tumor cells [20,21]. He et al. [22] confirmed that ginsenoside Rb1 treatment alleviated CIRI-induced behavioral defects, reduced pathological damage to brain tissue, and had neuroprotective effects. Similarly, kaempferol in ginseng has pharmacological effects, such as antioxidant, anti-inflammatory and antiapoptotic effects, and has high medicinal value, showing protective effects on brain injury-related diseases [23]. Yuan et al. [24] reported that kaempferol inhibits neuronal apoptosis, improves neuronal injury, and protects against brain injury in cerebral ischemia reperfusion rats. Betulin is a pentacyclic triterpenoid with pharmacological uses, such as anti-inflammatory and antioxidant effects. Studies have shown that betulin significantly improves learning memory and spatial cognition in rats and has antiapoptotic and hippocampal neuron protection effects in a dementia model in rats [25,26]. Notably, in this study, the above chemical ingredients were screened from the alcohol extract of KXS, which revealed the chemical basis of KXS in the treatment of VaD.

The hippocampus is an important brain region for learning and memory and plays an irreplaceable role in the processing pathway of memory information [27]. It has been shown that mice with damaged hippocampi have cured atrophy of neuronal cells in the CA1 area and low learning memory function [28]. Similarly, we observed that the hippocampal CA1 area of the model rats was severely damaged, with fewer neuronal cells and a sparsely disorganized arrangement compared with those of the control group. After KXS intervention, pathological damage in the hippocampal CA1 region of rats was significantly increased, the number of neurons was significantly increased, and the arrangement was tight and orderly, indicating that KXS could alleviate pathological damage in the hippocampal CA1 region of VaD rats. The Morris water

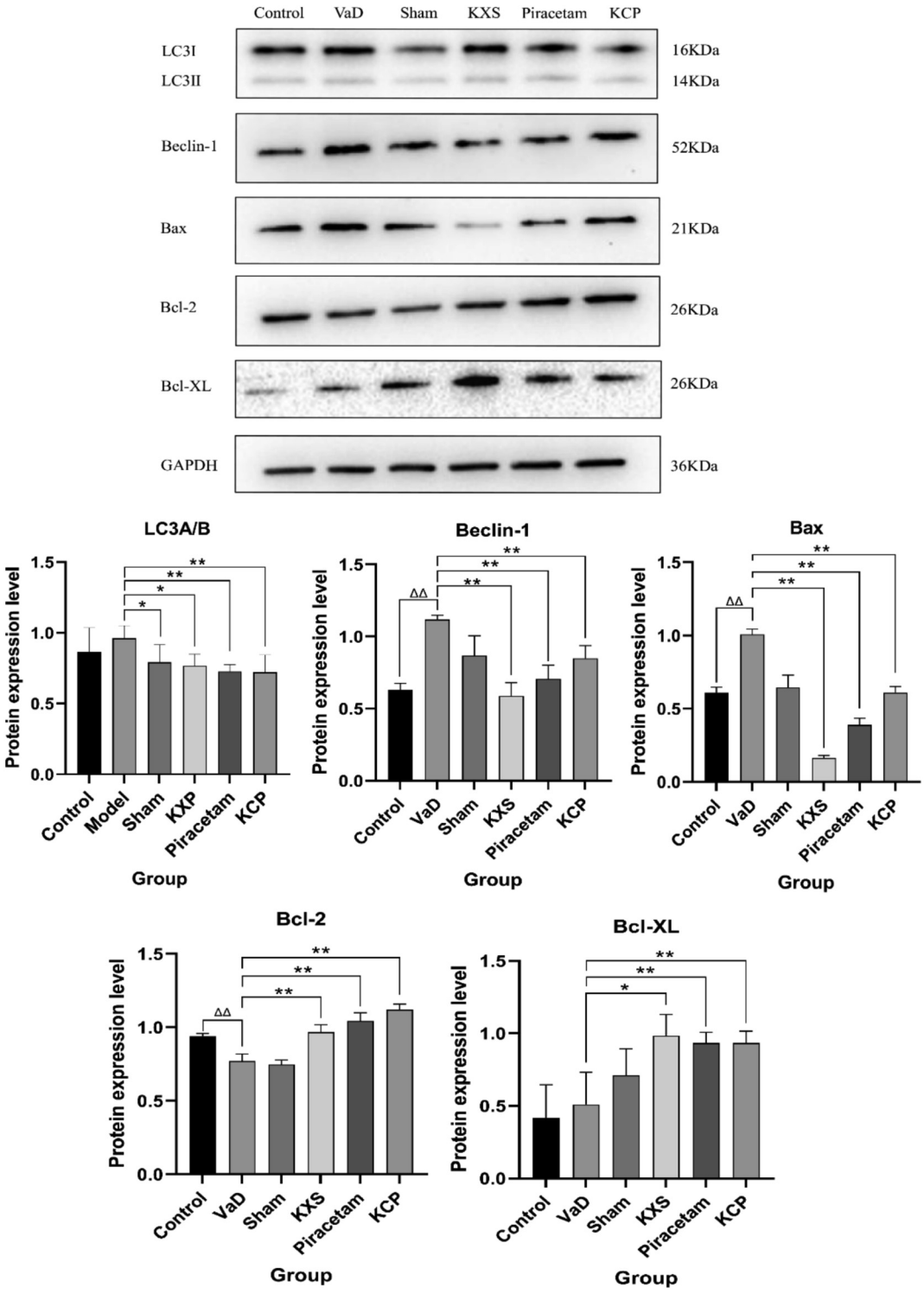

Fig. 4. Effects of KXS on LC3A/B, Beclin-1, Bax, Bcl-2 and Bcl-XL levels in rat brain tissue. (Compared with the control group, $^{\Delta\Delta}$ indicates $p < 0.01$; compared with the VaD group, * indicates $p < 0.05$ and ** indicates $p < 0.01$).

maze test is mainly used to test the learning and memory ability of animals. The results of this study revealed that the escape latency of the VaD model group was significantly greater than that of the control group, and the time spent in the target quadrant and the number of platform crossings were significantly lower. These findings indicate that the learning and memory ability of the VaD model group was significantly shorter than that of the VaD model group, whereas the escape latency of the KXS group was significantly shorter than that of the VaD model group. The time spent in the target quadrant and the number of platform crossings

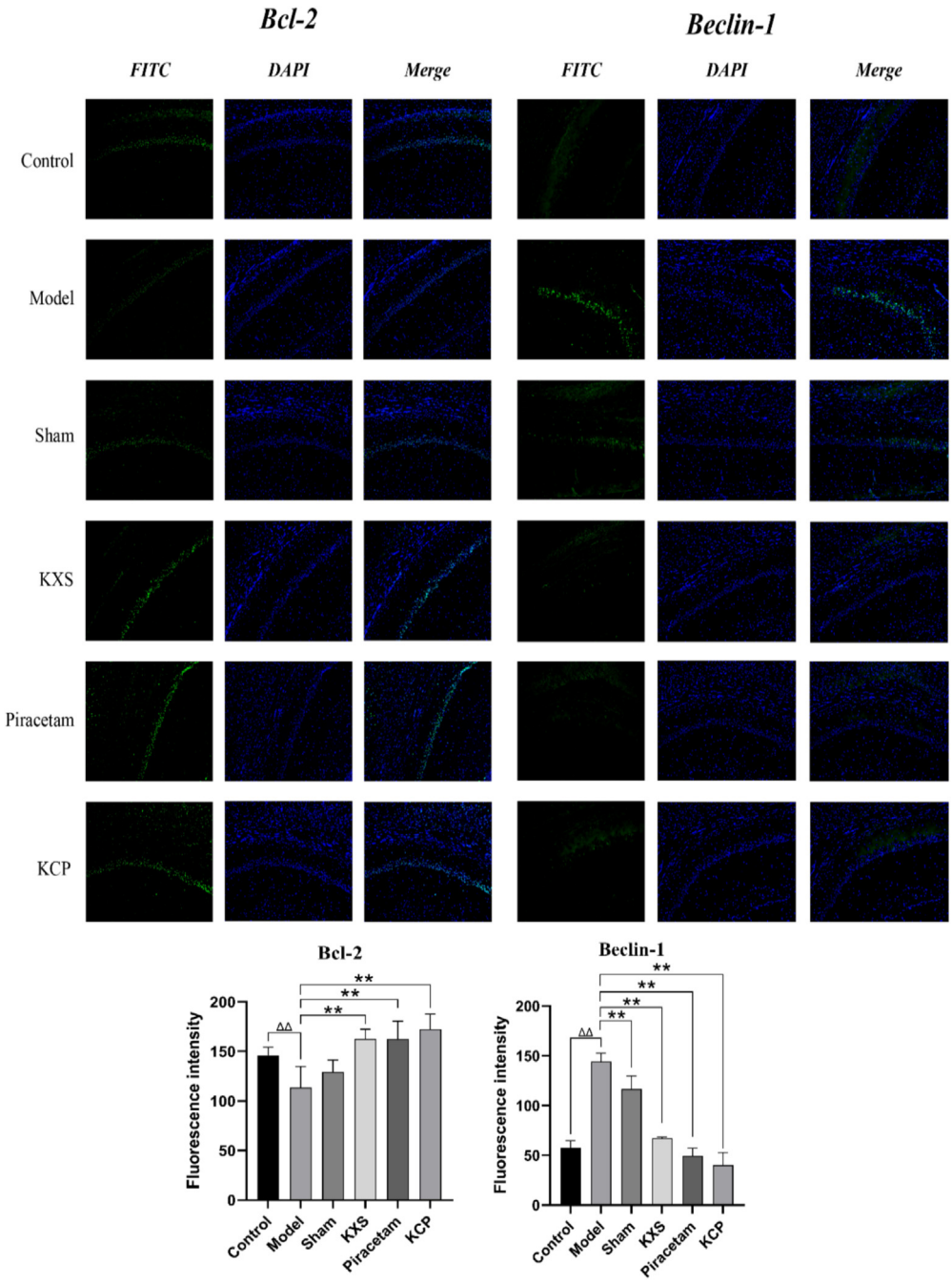

Fig. 5. The fluorescence expression of Bcl-2 and Beclin-1 in rat brain tissue. (Compared with the control group, $^{\Delta\Delta}$ indicates $p < 0.01$; compared with the VaD group, ** indicates $p < 0.01$).

increased significantly, indicating that KXS can improve the learning and memory ability of VaD rats.

Autophagy is a process in which some proteins and organelles in cells are encapsulated and dissolved by autolysosomes, and it is a programmed cell death mode [29]. Inhibition of autophagy is a potential target for the treatment of VaD, and it has been reported that inhibition of autophagy may favor synaptic remodeling in the CA1 area of the hippocampus of vascular dementia rats, promote neuronal survival, and thus improve the symptoms of dementia [30]. LC3A/B and Beclin-1 are often used as the main indicators for detecting the level of autophagy [31]. Our study showed that the protein expression levels of LC3A/B and Beclin-1 were elevated in the brains of VaD rats, which is consistent with the results of previous studies. After administration, the proteins expression levels of LC3A/B and Beclin-1 significantly decrease. Further, it was proved through immunofluorescence that Kaixin San can inhibit autophagy in cells. This can be explained by the mechanism of Kaixin San in treating VaD.

Our network pharmacology analysis demonstrated that active components in Kaixin San, including quercetin and kaempferol, exert therapeutic effects on VaD through critical targets such as Bcl-2. Furthermore, GO enrichment analysis revealed that positive

Table 1
KXS active ingredients screened from TCMSP database.

Source	Mol ID	Mol name	ID
Poria	MOL000282	ergosta-7,22E-dien-3beta-ol	FL1
	MOL000283	Ergosterol peroxide	FL2
	MOL000296	Hederagenin	FL3
Ginseng	MOL002879	Diop	RS1
	MOL000449	Stigmasterol	RS2
	MOL000358	beta-sitosterol	RS3
	MOL003648	Inermin	RS4
	MOL000422	Kaempferol	RS5
	MOL005308	Aposiopolamine	RS6
	MOL005317	Deoxyharringtonine	RS7
	MOL005318	Dianthramine	RS8
	MOL005320	Arachidonate	RS9
	MOL005321	Frutinone A	RS10
	MOL005344	ginsenoside rh2	RS11
	MOL005348	Ginsenoside-Rh4_qt	RS12
	MOL005356	Girinimbin	RS13
	MOL005376	Panaxadiol	RS14
	MOL005384	Suchilactone	RS15
	MOL005399	alexandrin_qt	RS16
	MOL000787	Fumarine	RS17
Polygalae Radix	MOL005321	Frutinone A	YZ1
	MOL009622	Fucosterol	YZ2
Acori Tatarinowii Rhizoma	MOL003542	8-Isopentenyl-kaempferol	SCP1
	MOL003576	(1R,3aS,4R,6aS)-1,4-bis(3,4-dimethoxyphenyl)-1,3,3a,4,6,6a-hexahydrofuro[4,3-c]furan	SCP2
	MOL003578	Cycloartenol	SCP3
	MOL000422	Kaempferol	SCP4

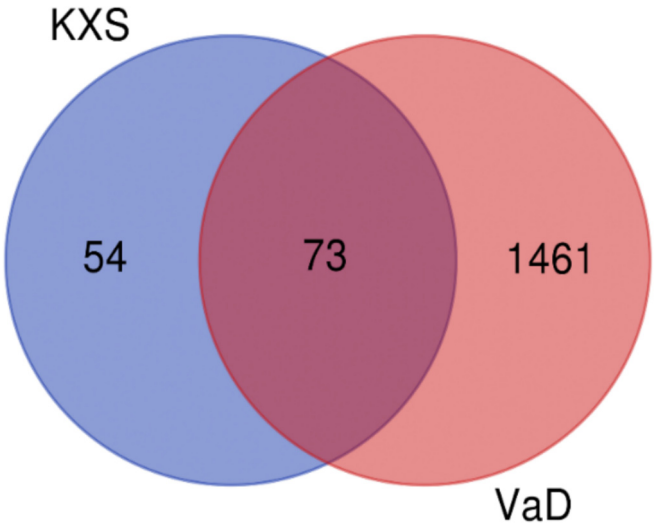

Fig. 6. Venn diagram of KXS active ingredient targets and VaD disease targets.

regulation of apoptotic processes plays a pivotal role in the anti-VaD mechanisms. Neuroapoptosis is a process of programmed cell death regulated by genes, and several studies have found that neuroapoptosis is closely related to the occurrence and development of VaD, so protection of neuronal cells and inhibition of neuroapoptosis are expected to be an important means of preventing and controlling VaD [32,33]. Pro-apoptotic proteins such as Bax and anti-apoptotic proteins such as Bcl-2 and Bcl-XL are apoptotic genes of cells, and studies have shown that the high and low levels of Bcl-2 and Bax expression are directly correlated with cell apoptosis [34]. Our study showed that vascular dementia rats had elevated levels of Bax expression and decreased levels of Bcl-2 and Bcl-XL expression in the brain, while after administration, the level of Bax expression in the brain of the rats was significantly reduced, and the levels of Bcl-2 and Bcl-XL expression were elevated. In addition, the fluorescence intensity of Bcl-2 demonstrated a significant elevation. These findings suggest that Kaixin San exerts inhibitory effects on apoptosis.

Both Bcl-2 and Beclin1 are recognized as regulatory genes involved in the modulation of apoptosis and autophagy, and their interaction is understood to influence autophagic function [35]. Bcl-2, a key apoptotic regulatory protein, directly regulates autophagic activity through its binding state with the autophagy protein Beclin-1. Under physiological conditions, the induction of autophagy by Beclin1 is inhibited by the binding of Bcl-2 to its BH3 domain [36,37]. Conversely, under ischemic stress, dissociation of phosphorylated Bcl-2 from Beclin-1 is observed. The released Beclin-1 then recruits ATG proteins to form complexes, promoting the conversion of LC3-I to LC3-II and initiating autophagosome formation [38]. In this study, Bcl-2 expression was significantly upregulated and LC3A/B expression was downregulated by KXS. This suggests that the Bcl-2/Beclin-1 interaction may be enhanced by KXS, thereby inhibiting excessive autophagy and apoptosis. This mechanism is supported by the findings of Dong et al. [39], where in a brain injury model, neuronal death caused by excessive autophagy activation was blocked by the Bcl-2/Beclin-1 interaction. Furthermore, a reduction in LC3 puncta formation and an improvement in cognitive function were demonstrated with the autophagy inhibitor 3-MA.

Moreover, pathways identified through network pharmacology screening – namely, 'Lipid and atherosclerosis', 'Fluid shear stress and atherosclerosis', 'AGE-RAGE signaling pathway in diabetic complications', 'IL-17 signaling pathway', and 'TNF signaling pathway' – are clearly associated with vascular dysfunction, chronic inflammation, and metabolic disturbances. These factors are considered the core drivers of VaD pathogenesis [40]. Neuronal damage and cognitive impairment in VaD are caused by cerebrovascular pathologies (including atherosclerosis, endothelial damage, and chronic hypoperfusion) and concomitant systemic/local inflammatory responses. These core pathological factors are potent inducers of excessive neuronal autophagy and apoptosis [41]. It was predicted by our network pharmacology approach that KXS improves vascular function and suppresses inflammatory responses through modulation of the relevant pathways mentioned above, representing regulation of upstream drivers. Furthermore, the observations from our animal experiments, where KXS significantly up-regulated Bcl-2 and down-regulated Beclin-1 and LC3A/B, thereby inhibiting neuronal hyperautophagy and apoptosis and improving cognitive function, provide direct evidence of the downstream protective effects resulting from intervention in these upstream pathways.

5. Conclusions

KXS has certain therapeutic effects on VaD model rats, and its possible mechanism of action is related to the regulation of LC3A/B, Beclin-1, Bax, Bcl-2, and Bcl-XL signaling factors to inhibit autophagy and delay apoptosis, improve the morphology of hippocampal tissues, repair the neural damage caused by VaD, and thus protect brain tissues. This study investigated the active ingre-

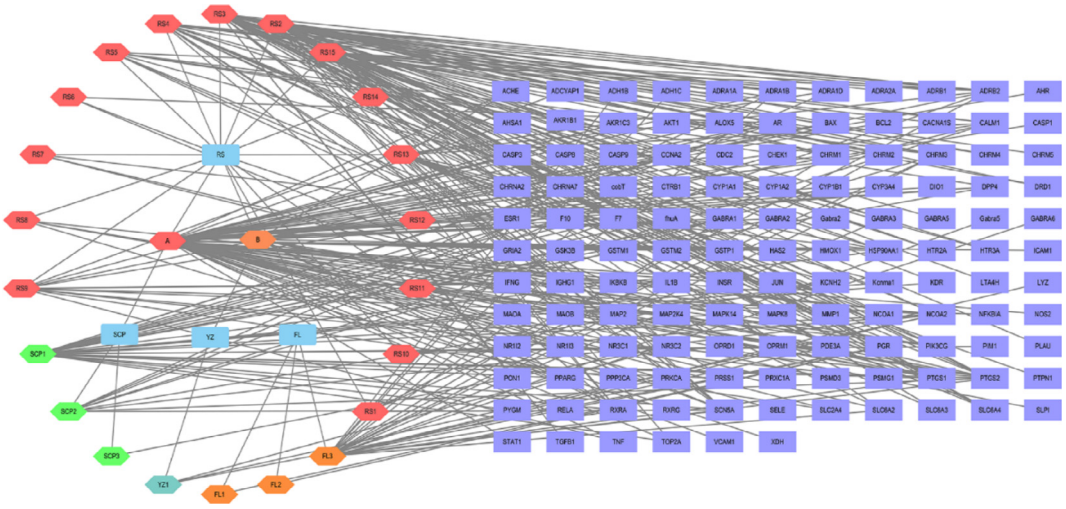

Fig. 7. The "active ingredient-target" network diagram of KXS in the treatment of VaD.

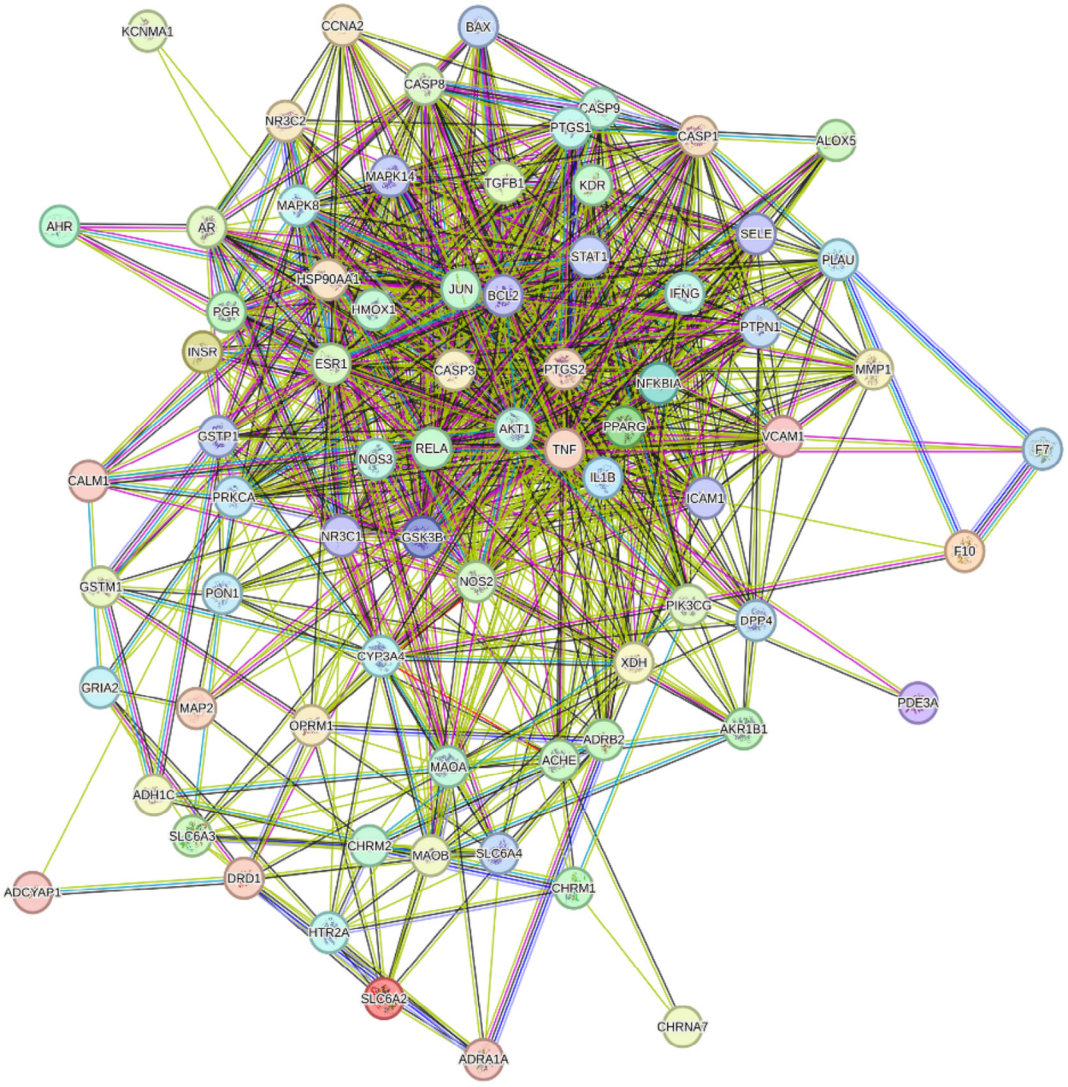

Fig. 8. Protein-protein interaction network diagram.

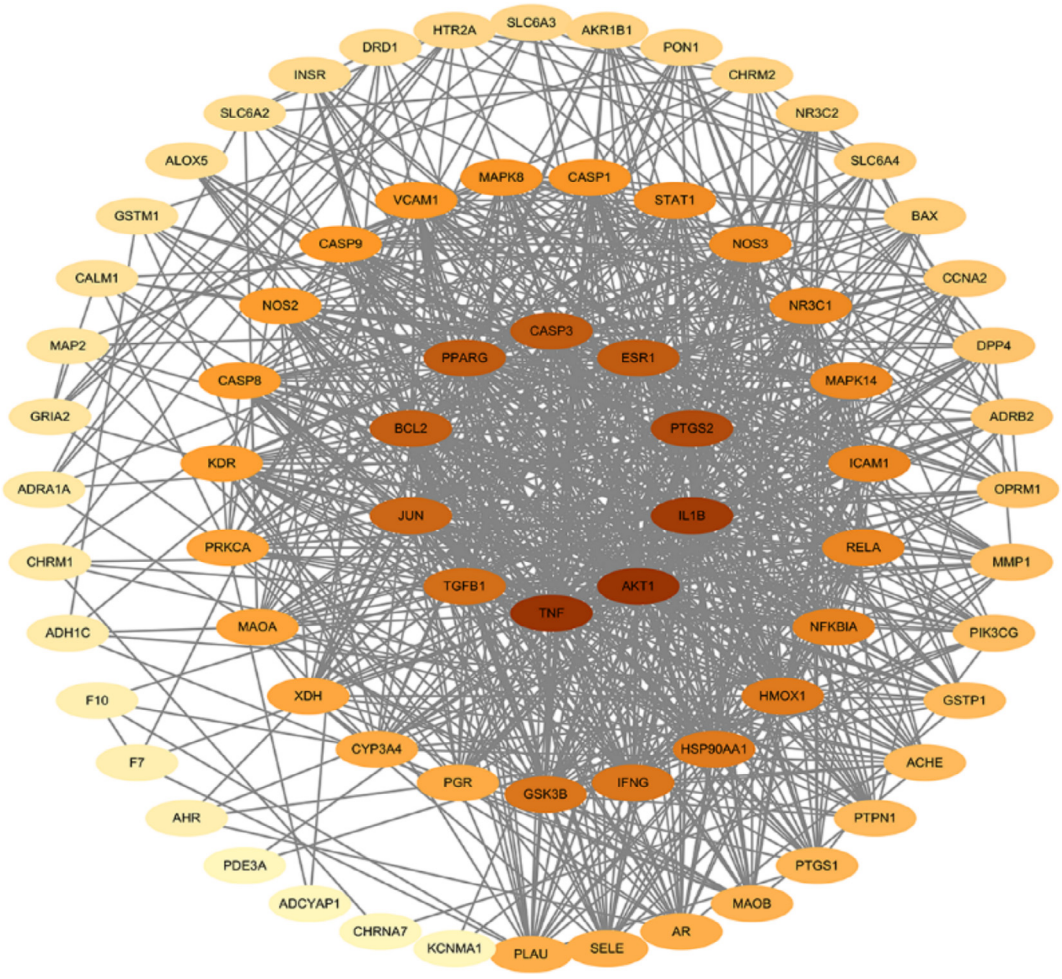

Fig. 9. Protein-protein interaction core targets diagram.

dients, target genes and related signaling pathways associated with VaD treatment via Happy dispersal through a network pharmacology approach, providing a theoretical basis for more in-depth experimental studies. However, there are still some shortcomings in this study. For example, the composition of KXS is complex, so further exploration of the material basis of its treatment of VaD is necessary. Network pharmacology is a prediction method that is based on big data and has limitations. The exact mechanism of KXS in the treatment of VaD needs to be further studied to better guide its clinical application.

CRediT authorship contribution statement

Meng-qi Li: Writing – review & editing, Writing – original draft, Methodology, Investigation, Formal analysis, Conceptualization. **Yu-cheng Lu:** Writing – review & editing, Visualization, Validation, Investigation, Formal analysis. **Yan-chun Li:** Writing – review & editing, Visualization, Validation, Investigation, Formal analysis. **Yu-fu Zeng:** Validation, Investigation. **Ying-ying Cao:** Methodology, Investigation. **Ling Zhang:** Supervision, Project administration, Methodology, Funding acquisition, Conceptualization. **Ben Chen:** Methodology, Investigation. **Ling Chen:** Methodology, Investigation. **Wei-an Qiu:** Investigation. **Zi-heng Huang:** Investigation.

Ethical approval (animals)

All animal experiments were reviewed and approved by the Guangxi University of Chinese Medicine Institutional Animal Ethical and Welfare Committee and were carried out under the Guidelines for Animal Experiments at the Guangxi University of Chinese Medicine. Animal Ethics Approval number: DW20211210-205.

Financial support

This work was supported by The Open Project of Guangxi Health Commission Guangxi Key Laboratory of Molecular Biology of Preventive Medicine of Traditional Chinese Medicine (GXHCMBTCM-06); Scientific research project of Education Department of Guangxi Zhuang Autonomous Region (YB2014172; JGY2024210). Innovation Project of Guangxi Graduate Education of GXUCM (YCSY2025083).

Declaration of competing interests

All the authors declared that they had no conflicts to do the work.

Acknowledgements

We would like to thank thanks to all the databases and websites mentioned in this manuscript

Supplementary material

https://doi.org/10.1016/j.ejbt.2025.08.001.

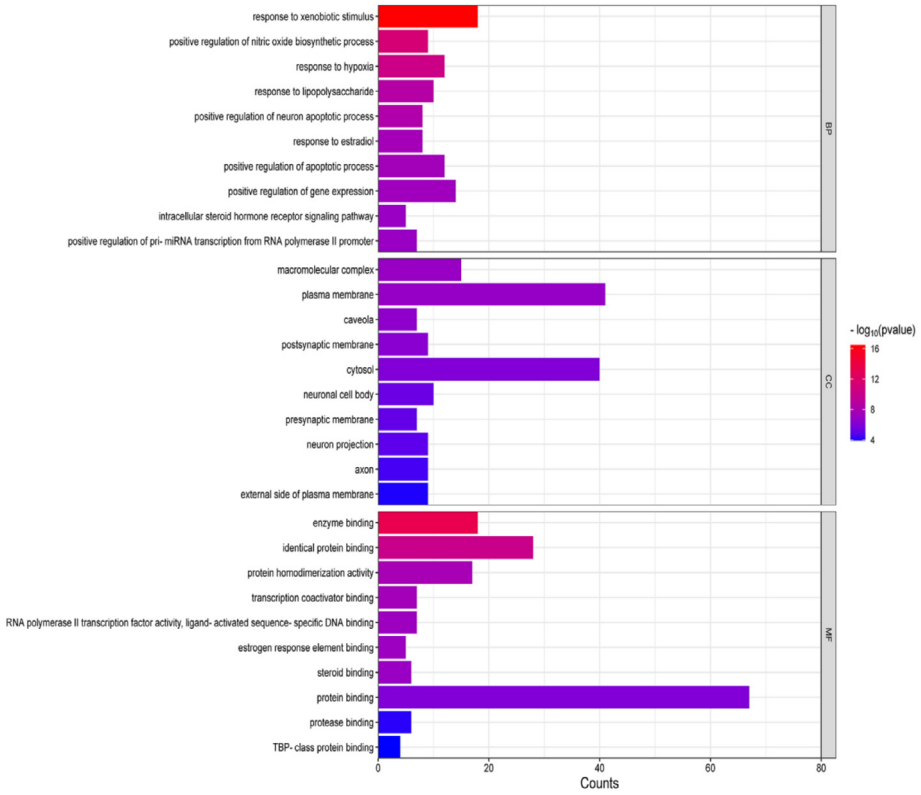

Fig. 10. GO function histogram of KXS therapy for VaD.

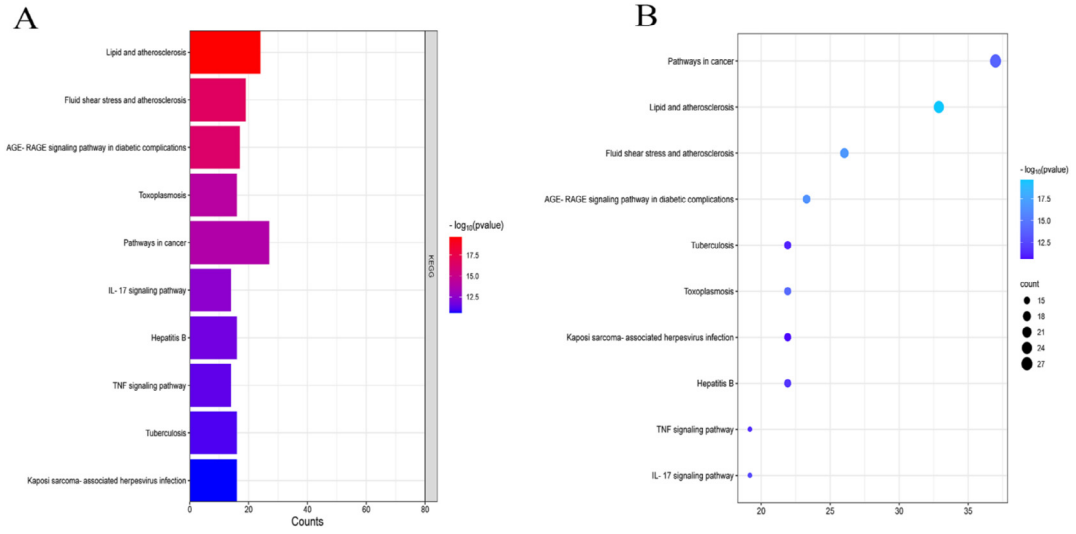

Fig. 11. Enrichment results of KEGG pathway. (A) KEGG pathway histogram in KXS treatment of VaD. (B) Bubble map of KEGG pathway in KXS treatment of VaD.

Data availability

All data generated or analyzed in this study are included in this article and its additional files. Some of the data are available in the TCMSP, UniProt, GeneCards, STRING and Metascape database.

References

[1] Liu H, Zhao C. Research progress of traditional Chinese and Western medicine in vascular dementia. Mod J Integr Tradit Chin West Med 2021;30(3):334–8.
[2] Yokota RT, Berger N, Nusselder WJ, et al. Contribution of chronic diseases to the disability burden in a population 15 years and older, Belgium, 1997-2008. BMC Public Health 2015;15:229. https://doi.org/10.1186/s12889-015-1574-z. PMid: 25879222.
[3] Yufen T. The latest trends and trends of China's population: Analysis of data from the 7th National Census. J China Inst Ind Relat 2021;35(4):15–25.
[4] Battistin L, Cagnin A. Vascular cognitive disorder. A biological and clinical overview. Neurochem Res 2010;35(12):1933–8. https://doi.org/10.1007/s11064-010-0346-5. PMid: 21127967.
[5] Liu F, Niu K, Wu Z, et al. Effects of Jiji decoction on the cognitive function and oxidative stress in mice with vascular dementia induced by cerebral ischemia/reperfusion. Chin J Appl Physiol 2015;31(2):170–3. PMid: 26248428.
[6] Sun S, Lu ZL. Essential prescriptions worth a thousand gold for urgent cases. Shenyang: Liaoning Science and Technology Press; 1997.
[7] Wang J, Zhou X, Hu Y, et al. Research progress on pharmacodynamic material basis and pharmacological action mechanism of Kai-Xin-San. Chin Tradit Herb Drug 2020;51(18):4780–8.

[8] Yang J, Liu Y. Efficacy observation of Kaixin powder mixture on vascular dementia. Shanxi J Tradit Chin Med 2023;39(9):30–2. https://doi.org/10.20002/j.issn.1000-7156.2023.09.010.
[9] Sun Y, Sun T, Li M, et al. Study on modern pharmacological action and mechanism of action of Kaixinsan. Chin J Basic Med Tradit Chin Med 2021;27(4):650–4. https://doi.org/10.19945/j.cnki.issn.1006-3250.2021.04.030.
[10] Zhao X, Liu J, Yang S, et al. Ling-Yang-Gou-Teng-decoction prevents vascular dementia through inhibiting oxidative stress induced neurovascular coupling dysfunction. J Ethnopharmacol 2018;222:229–38. https://doi.org/10.1016/j.jep.2018.03.015. PMid: 29545211.
[11] Liu S, He Y, Shi J, et al. Allicin attenuates myocardial ischemia reperfusion injury in rats by inhibition of inflammation and oxidative stress. Transpl Proc 2019;51(6):2060–5. https://doi.org/10.1016/j.transproceed.2019.04.039. PMid: 31399184.
[12] Lu YC, Li MQ, Zhang L, et al. Wuzang Wenyang Huayu Tang promoting learning-memory ability in vascular dementia rats via brain-gut-microbiome axis. Pharmacol Res Mod Chin Med 2023;7:100259. https://doi.org/10.1016/j.prmcm.2023.100259.
[13] Zhao Y, Wu J, Li D, et al. Human ESC-derived immunity- and matrix- regulatory cells ameliorated white matter damage and vascular cognitive impairment in rats subjected to chronic cerebral hypoperfusion. Cell Prolif 2022;55(5):e13223. https://doi.org/10.1111/cpr.13223. PMid: 35437845.
[14] Du SQ, Wang XR, Zhu W, et al. Acupuncture inhibits TXNIP-associated oxidative stress and inflammation to attenuate cognitive impairment in vascular dementia rats. CNS Neurosci Ther 2018;24(1):39–46. https://doi.org/10.1111/cns.12773. PMid: 29110407.
[15] Ning H, Cao D, Wang H, et al. Effects of haloperidol, olanzapine, ziprasidone, and PHA-543613 on spatial learning and memory in the Morris water maze test in naïve and MK-801-treated mice. Brain Behavior 2017;7(8):e00764. https://doi.org/10.1002/brb3.764. PMid: 28828223.
[16] Yu W, Yin H, Sun Y, et al. The attenuation effect of potassium 2-(1-hydroxypentyl)-benzoate in a mouse model of diabetes-associated cognitive decline: The protein expression in the brain. CNS Neurosci Ther 2022;28(7):1108–23. https://doi.org/10.1111/cns.13847. PMid: 35445545.
[17] Xu X, Zhang W, Huang C, et al. A novel chemometric method for the prediction of human oral bioavailability. Int J Mol Sci 2012;13(6):6964–82. https://doi.org/10.3390/ijms13066964. PMid: 22837674.
[18] Lu W, Zhang S, Shen S, et al. Research progress in pharmacological effects and pharmacokinetics of ginsenoside Rc. Chin Tradit Herb Drug 2018;49(24):5961–7. https://doi.org/10.7501/j.issn.0253-2670.2018.24.033.
[19] Wang S, Jin J. Advances of the main chemical ingredients and isolation methods in ginseng. Ginseng Res 2019;31(3):54–7. https://doi.org/10.19403/j.cnki.1671-1521.2019.03.014.
[20] An H, Li S, Gao Y, et al. Ginsenoside Rg3 synergistically promotes apoptosis of lung cancer H358 cells with TRAIL and its mechanism. Chin J Cancer Biother 2019;26(9):988–92.
[21] Bai L, Chen C, Li Z, et al. Effects of genoside Rh2 on the apoptosis of human brain glioma cells U87MG. Chin J Clin Neurosurg 2019;24(3):155–8. https://doi.org/10.13798/j.issn.1009-153X.2019.03.010.
[22] He H, Yang Y, Zhang X, et al. Regulation of Nrf2/A20/eEF1A2 axis by ginsenoside Rb1: A key pathway in alleviating cerebral ischemia-reperfusion injury. Discov Med 2024;36(187):1743–57. https://doi.org/10.24976/Discov.Med.202436187.160. PMid: 39190389.
[23] Bian Y, Dong Y, Sun J, et al. Protective effect of kaempferol on LPS-induced inflammation and barrier dysfunction in a coculture model of intestinal epithelial cells and intestinal microvascular endothelial cells. J Agric Food Chem 2020;68(1):160–7. https://doi.org/10.1021/acs.jafc.9b06294. PMid: 31825618.
[24] Yuan Y, Xia F, Gao R, et al. Kaempferol mediated AMPK/mTOR signal pathway has a protective effect on cerebral ischemic-reperfusion injury in rats by inducing autophagy. Neurochem Res 2022;47(8):2187–97. https://doi.org/10.1007/s11064-022-03604-1. PMid: 35524892.
[25] Ma Z, Jia YG, Zhu XX. Glycopolymers bearing galactose and betulin: Synthesis, encapsulation, and lectin recognition. Biomacromolecules 2017;18(11):3812–8. https://doi.org/10.1021/acs.biomac.7b01106. PMid: 28982003.
[26] Jin Y, Fu Z, Lin Z, et al. Effect of betulin on the expression of APH-1 and PEN-2 in hippocampal neurons of Alzheimer's model rats. J Tianjin Univ Tradit Chin Med 2021;40(3):384–8.
[27] Su K, Lyu Z, Wu M, et al. Effect of electroacupuncture on BDNF/TrkB/PI3K/Akt pathway and hippocampal neuronal protection in rats with learning and memory impairment after ischemia reperfusion. Chin Gen Pract 2023;26(33):4187–93.
[28] Yuan H, Zhu M, Wang Y, et al. Effects of astragaloside IV on behavior and hippocampus of mice with memory impairment. Shaanxi J Tradit Chin Med 2023;44(7):843–8.
[29] Huett A, Goel G, Xavier RJ. A systems biology viewpoint on autophagy in health and disease. Curr Opin Gastroenterol 2010;26(4):302–9. https://doi.org/10.1097/MOG.0b013e32833ae2ed. PMid: 20571384.
[30] Zhang W, Liu J, Liu B, et al. Effects of autophagy on expression of growth-associated protein- 43 and microtubule associated protein- 2 in CA1 area of hippocampus of vascular dementia rats. Chin J Rehabil Theory Pract 2016;22(7):745–9.
[31] Fleming A, Bourdenx M, Fujimaki M, et al. The different autophagy degradation pathways and neurodegeneration. Neuron 2022;110(6):935–66. https://doi.org/10.1016/j.neuron.2022.01.017. PMid: 35134347.
[32] Zhao T, Fu Y, Sun H, et al. Ligustrazine suppresses neuron apoptosis via the Bax/Bcl-2 and caspase-3 pathway in PC12 cells and in rats with vascular dementia. IUBMB Life 2018;70(1):60–70. https://doi.org/10.1002/iub.1704. PMid: 29247598.
[33] Wang D, Wang Y, Shan M, et al. Apelin receptor homodimer inhibits apoptosis in vascular dementia. Exp Cell Res 2021;407:112739. https://doi.org/10.1016/j.yexcr.2021.112739. PMid: 34343559.
[34] Huang X, Chen Q, Ren Y. Effects of puerarin on the expressions of Bcl-2, Bax and Caspase-3 in the motor cortex of mice with traumatic brain injury. Clin J Chin Med 2019;11(25):13–5.
[35] Maejima Y, Kyoi S, Zhai P, et al. Mst1 inhibits autophagy by promoting the interaction between Beclin1 and Bcl-2. Nat Med 2013;19:1478–88. https://doi.org/10.1038/nm.3322. PMID: 24141421.
[36] Sinha S, Levine B. The autophagy effector Beclin 1: A novel BH3-only protein. Oncogene 2008;27:(Suppl 1):S137–48. https://doi.org/10.1038/onc.2009.51. PMid: 19641499.
[37] Kim YH, Kwak MS, Shin JM, et al. Inflachromene inhibits autophagy through modulation of Beclin 1 activity. J Cell Sci 2018;131(4):jcs211201. https://doi.org/10.1242/jcs.211201. PMid: 29361549.
[38] Wu Y, Li Z, Ding T, et al. Bidirectional regulation of neuronal autophagy in ischemic stroke: Mechanisms and therapeutic potential. Ageing Res Rev 2025;111:102842. https://doi.org/10.1016/j.arr.2025.102842. PMid: 40706815.
[39] Dong X, Liang Q, Pan YZ, et al. Novel Bcl-2 inhibitors selectively disrupt the autophagy-specific Bcl-2-Beclin 1 protein-protein interaction. ACS Med Chem Lett 2022;13(9):1510–6. https://doi.org/10.1021/acsmedchemlett.2c00309. PMid: 36105331.
[40] Li M, An Y. Vascular dementia research progress of the pathogenesis of cerebrovascular disease. J Chronic Epidemiol Mag 2023;24(5):697–9. https://doi.org/10.16440/J.CNKI.1674-8166.2023.05.12.
[41] Yu Z, Wang H, Xu F, et al. Study on the mechanism of medicated serum containing Shengi Maixintong Capsule regulating macrophage autophagy against atherosclerosis through AMPK/mToR pathway. J Changchun Univ Chin Med 2025;41(7):756–61. https://doi.org/10.13463/j.cnki.cczyy.2025.07.011.